Supporting Information
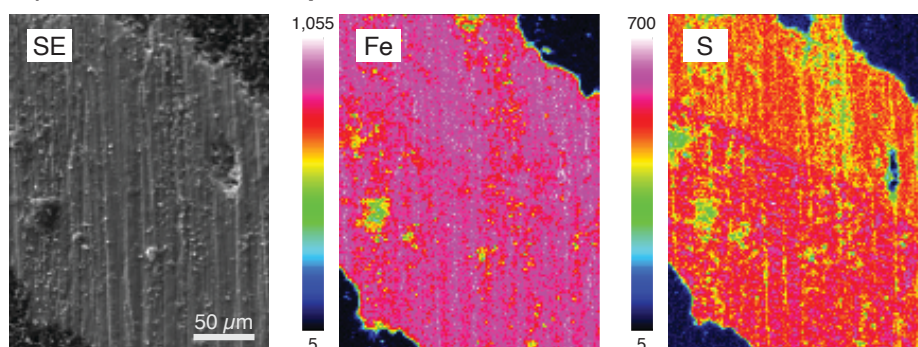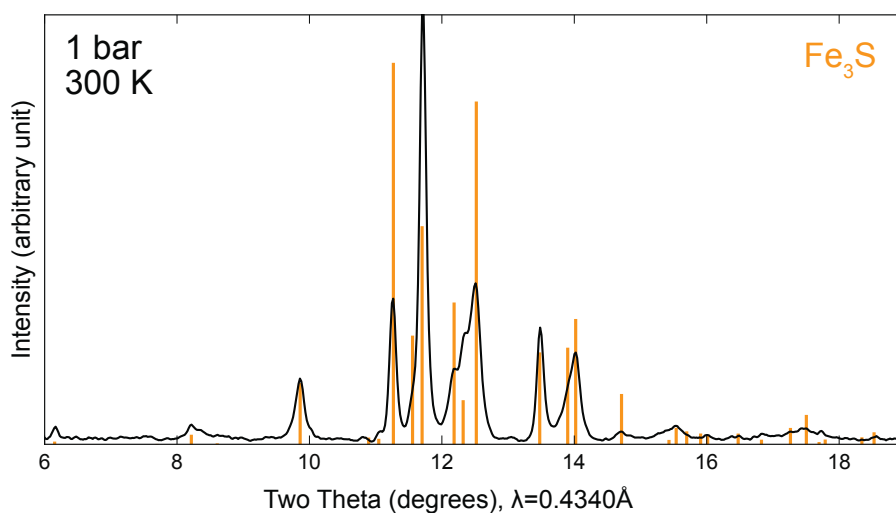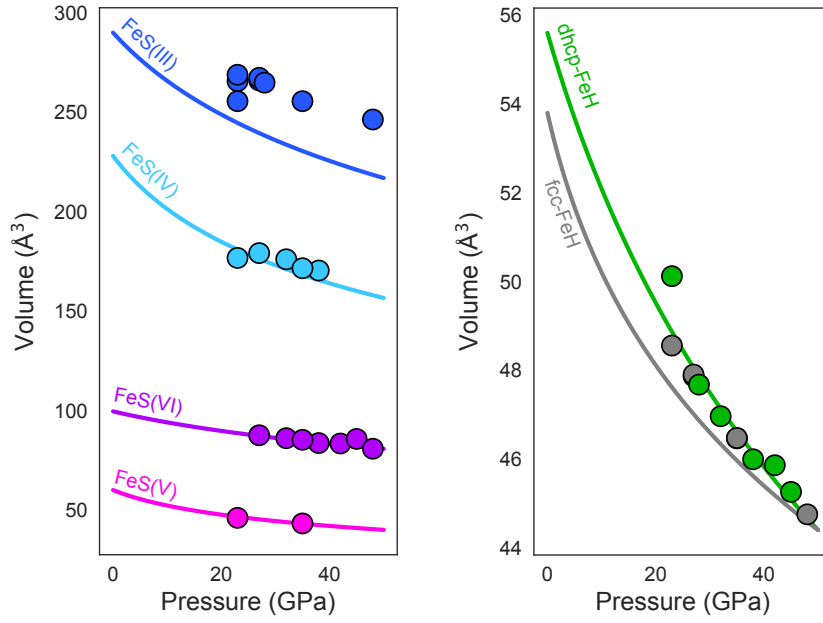
a) Chemical maps
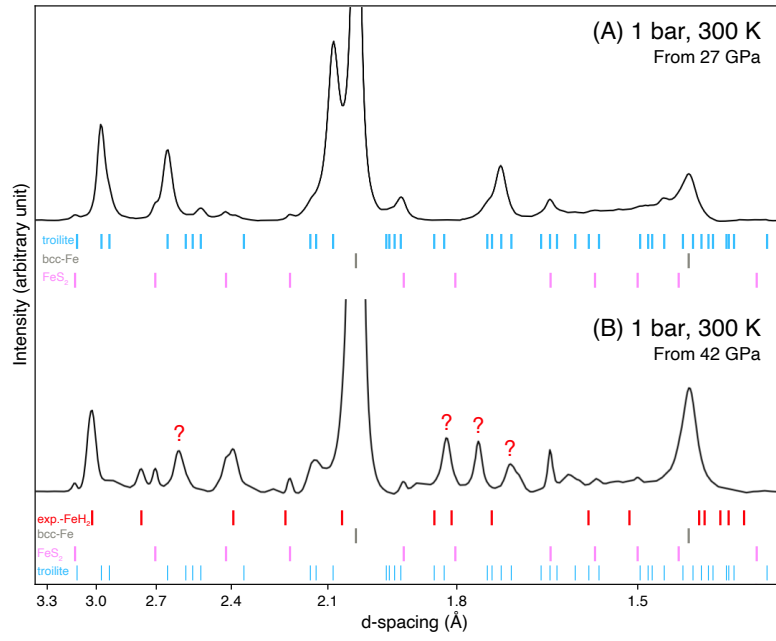

b) XRD

Fig. S1. Scanning electron microscopy (SEM) and X-ray diffraction (XRD) data for pure Fe_3S synthesized in the multi-anvil press. (a) Secondary electron image and corresponding iron and sulfur WDS maps showing homogeneity of the sample for both chemical elements. Some areas with different colors in the compositional maps are from surface roughness of the unpolished cross sectional areas of the multi-anvil press sample. Point analyses in those areas give similar Fe and S compositions (see Table S1. (b) XRD for this sample shows pure Fe_3S.

Fig. S2. The unit-cell volumes of FeS(III), FeS(IV), FeS(V) and FeS(VI) laser-heated in a H medium in this study (the colored circles). The colored lines represent equations of state of the same phases from the literature [FeS(III): *Kusaba et al.* [1997]; FeS(IV) and FeS(V): *Urakawa et al.* [2004]; FeS(VI): *Ono and Kikegawa* [2006]; dhcp-FeH: *Pépin et al.* [2014]; fcc-FeH: *Narygina et al.* [2011]]. FeS(IV) shows a slight increase and FeS(III) shows a significant increase. Such increases in the unit-cell volume suggest the presence of H in the crystal structures.

Fig. S3. XRD diffraction patterns measured at 1 bar and 300 K after decompression. A) [Fe+Fe$_3$S] + H$_2$ reacted at 27 GPa. Troilite (FeS(I)), bcc-Fe and FeS$_2$ are present. B) [Fe+Fe$_3$S] + H$_2$ reacted at 42 GPa. Bcc-Fe and FeS$_2$ are present, as well as some new diffraction lines.

Tab. S1. Electron probe micro-analysis (EPMA) quantitative point analyses for the Fe$_3$S starting material synthesized in the multi anvil press. Uncertainty on the measurement is shown in parentheses. The data were obtained using wavelength dispersive spectroscopy (WDS). See text for details about the samples and microprobe analysis procedure.

Sample	max. T (K)	Phases	S (wt.%)	Fe (wt.%)	Total (wt.%)
BB1520	1533	Fe$_3$S	14.47 (4)	84.99 (11)	99.46
		Fe$_3$S	16.41 (4)	83.27 (10)	99.68

Tab. S2. **Experimental runs.** Uncertainties on the last digit(s) are shown in parenthesis.

Run #	Starting Material	Pressure (GPa)	Temperature range (K)
231e	Fe_3S	28(2)	2820
331e	Fe_3S	32(2)	1930–2580
431e	Fe_3S	37(3)	3130–3950
120–220	Fe_3S	38(3)	1692–4057
320	Fe_3S	45(3)	2281–3076
132a	FeS	23(2)	1892–2272
103b	FeS	35(2)	1791–4579
131c	$Fe-Fe_3S$	27(2)	1150–2670
231c–431c	$Fe-Fe_3S$	42(3)	1520–4437

Tab. S3.   X-ray diffraction data for the new phase (FeSH) at 38 GPa. Unit-cell volume parameters are: $a = b = 2.979(3)$ Å, $c = 10.401(13)$ Å and $\alpha = \beta = \gamma = 90°$. h, k, l are Miller indices, 2θ is the Bragg angle and d is the d-spacing. obs: observed; calc: calculated; diff: difference.

h	k	l	2θ-obs (degrees)	d-obs (Å)	d-calc (Å)	d-diff (Å)
1	0	1	6.7034	2.8599	2.8617	-0.0018
0	0	4	7.3781	2.5986	2.6017	-0.0031
1	0	3	8.4880	2.2593	2.2589	0.0004
1	1	4	11.717	1.6380	1.6363	0.0017

Tab. S4.   Volume difference between hcp-Fe (baseline) and different alloys (iron hydrides and iron sulfides). The corresponding volume increase caused by one atom of H was calculated and averaged over all Fe-rich alloys. The same analysis was performed for S.

Baseline	Alloy	ΔV (Å^3/Fe)	# of H or S per Fe	ΔV/(# of S or H) (Å^3/Fe)
hcp-Fe	dhcp-FeH	1.56	1.00	1.56
	FeH_2	3.82	2.00	1.91
	FeH_3	5.86	3.00	1.95
	FeH_5	10.05	5.00	2.01
hcp-Fe	Fe_3S	2.89	0.33	8.66
	Fe_2S	4.22	0.50	8.43
	FeS	9.86	1.00	9.86
	FeS_2	21.46	2.00	10.73